

Novel Porous Ceramic Material via Burning of Polylactide/Layered Silicate Nanocomposite

Suprakas Sinha Ray,[†] Kazuaki Okamoto,[‡] Kazunobu Yamada,[§] and Masami Okamoto^{*†}

Advanced Polymeric Materials Engineering, Graduate School of Engineering, Toyota Technological Institute, Hisakata 2-12-1, Tempaku, Nagoya 468 8511, Japan, Nagoya Municipal Research Institute, Rokuban 3-4-41, Atsuta, Nagoya 456-0058, Japan, and Unitika Ltd., Kozakura 23, Uji, Kyoto 611-0021, Japan

Received January 11, 2002; Revised Manuscript Received January 29, 2002

ABSTRACT

This letter describes the preparation and characterization of a novel porous ceramic material via the burning of the polylactide/layered silicate nanocomposite. WAXD patterns indicate that an amorphous structure was developed in the porous ceramic material after sintering the nanocomposite. SEM observation revealed a morphology in which individual silicate layers stacked together to form platelet structure and produce house of cards structure porous ceramic material. The stress–strain curve of the porous ceramic material shows elastic-like property in the elastic region ($\leq 8\%$ strain) under compression test.

Porous ceramic materials are increasingly found to have significant applications due to their unique set of properties, such as low density, low thermal conductivity, high-temperature stability, low dielectric constant, high permeability, and high resistance to chemical attack.¹ These attractive properties have allowed them to be used in diverse applications such as metal, hot gas, and ion-exchange filtration, thermal protection systems, heat exchangers, catalyst supports, and refractory linings.^{2–7} The most conventional method for porous ceramic material production included the immersion of an open-cell polymeric foam into a ceramic slurry with subsequent burning of the organic skeleton. This method led to some problems of low strength, leaving voids in the struts and resulting in cracks after the burnout of the polymer substrate.⁸

Recently, polymer/layered silicate nanocomposites have received significant research attention because they often exhibit physical and chemical properties that are dramatically different from their micro- and macrocomposite counterparts. In most of the cases, the research has generally proven that all types and classes of nanoscale materials lead to new and much improved materials properties.^{9,10} Very recently, a new

route for the preparation of porous ceramic materials from thermosetting epoxy/layered silicate nanocomposites was reported by Brown et al.¹¹ This route offers an attractive potential for the diversification and application of polymer/layered silicate nanocomposites. In a recent series of our ongoing studies on polymer/organically modified layered silicate (OMLS) nanocomposites, we prepared new nanocomposites of polylactide (PLA)¹² (abbreviated as PLACNs) with montmorillonite (MMT) intercalated with octadecylammonium cations.

In this paper, we report the results on the novel porous ceramic material via burning of the PLACN. In the PLACN containing 3.0 wt % inorganic clay (PLACN3), it appears from bright field transmission electron microscopy (TEM) observation (Figure 1A) that stuck silicate layers of about 450 nm length and about 38 nm thickness, which consist of about 13 parallel individual silicate layers that have an original thickness of ~ 1 nm and an average length of 150 nm, are finely dispersed in the PLA matrix.

On wide-angle X-ray diffraction (WAXD) of the same PLACN3 (Figure 1D), we still identified Bragg diffraction peaks resulting from 13 layers of ordered clay particles remaining in the PLACN3 due to the intercalation of PLA chains in the silicate galleries. The observed diffraction angle was $2\Theta \cong 2.91^\circ$ for the (001) plane, leading to the basal spacing of $d_{(001)} \cong 3.03$ nm, which is about 30% larger than

* To whom correspondence should be addressed. Tel: +81 52-809-1861. Fax: +81 52-809-1864. E-mail: okamoto@toyota-ti.ac.jp.

[†] Advanced Polymeric Materials Engineering, Graduate School of Engineering, Toyota Technological Institute.

[‡] Nagoya Municipal Research Institute.

[§] Unitika Ltd.

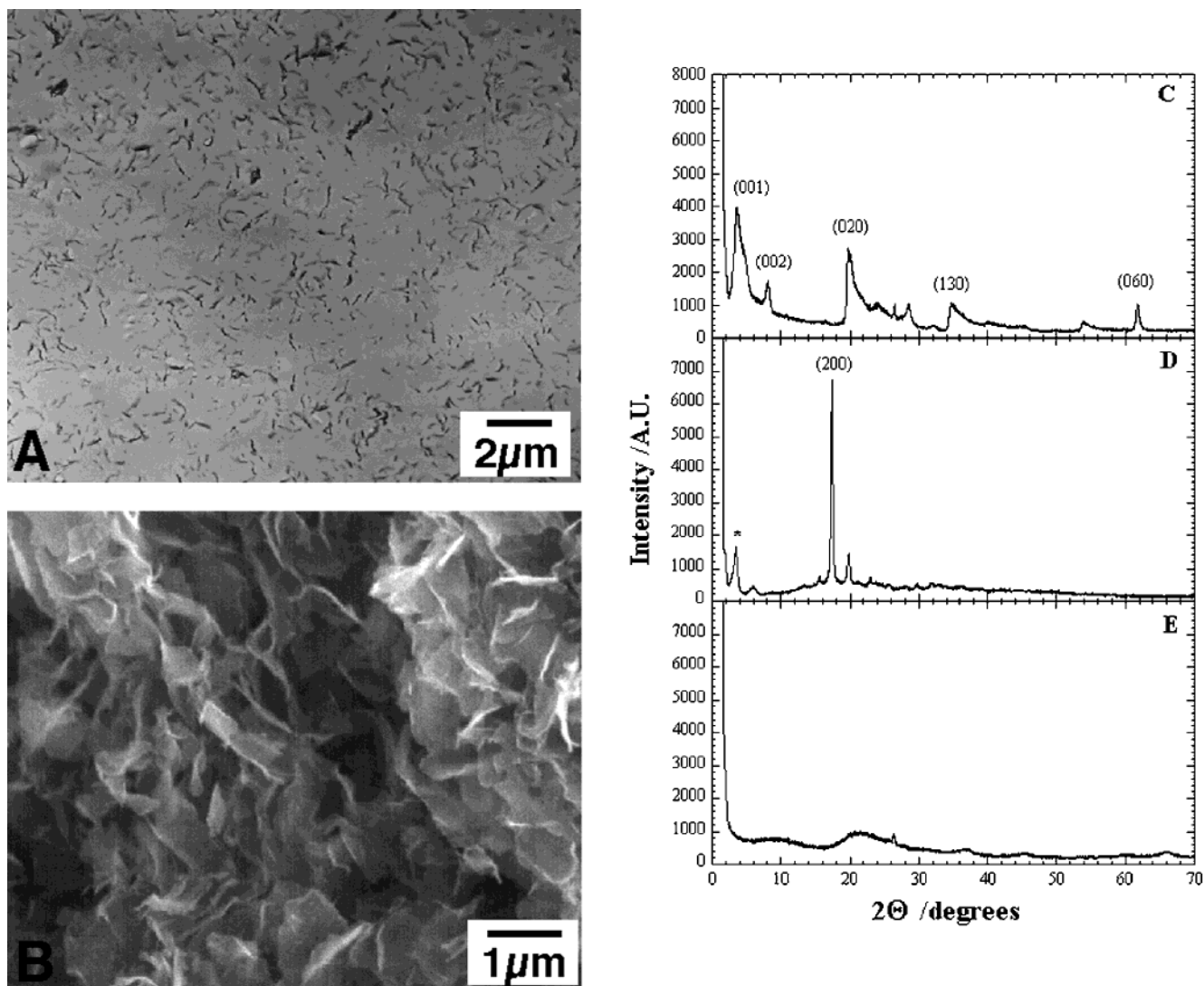


Figure 1. (A) TEM micrograph of PLACN3. The ultrathin section (edge of the compress sheets) with a thickness of 70 nm was microtomed at $-80\text{ }^{\circ}\text{C}$ using a Reichert Ultracut cryoultramicrotome without staining. (B) SEM image of porous ceramic material after coated with platinum layer ($\sim 10\text{ nm}$ thickness). (C) WAXD pattern of OMLS. (D) WAXD pattern of PLACN3. The asterisk indicates the position of (001) reflection for PLACN3. In this profile, the strong diffraction peak at $2\Theta \cong 17.63^{\circ}$ is assigned to the reflection of (200) plane of α -phase crystallite of PLA, which is pseudo orthorhombic with chains in a $-10/3$ helical conformation.¹³ (E) WAXD pattern of porous ceramic material.

that of the spacing, $d_{(001)} \cong 2.31\text{ nm}$ (calculated from $2\Theta \cong 3.82^{\circ}$) for the OMLS solid, as shown in Figure 1C.

Figure 1B shows a scanning electron microscope (SEM) image (JSM-5900, JEOL) of the fracture surface of the porous ceramic material prepared from the simple burning of a thick sheet of PLACN3 in a furnace, under air, at the heating rate of $10\text{ }^{\circ}\text{C min}^{-1}$. The temperature was initially brought up to $350\text{ }^{\circ}\text{C}$, then kept at that temperature for 1 h, and finally was raised to $950\text{ }^{\circ}\text{C}$. After the complete burning, as seen in Figure 1B, the PLACN3 becomes a white mass with a porous structure.¹⁴ The bright lines in the SEM image correspond to the edge of the stacked silicate layers. In the porous ceramic material, the silicate layers form a house of cards structure, which consists of large plates having a length of $\sim 1000\text{ nm}$ and thicknesses of $\sim 30\text{--}60\text{ nm}$. This implies that the further stacked platelet structure is formed during burning. The material exhibits open-cell type structure¹⁵ having a $100\text{--}1000\text{ nm}$ diameter void; a BET surface area,

measured by Autosorb-1 (Quantachrome Corp.), of $31\text{ m}^2\text{ g}^{-1}$; and a low density of porous material, 0.187 g ml^{-1} , estimated by the buoyancy method. The BET surface area value of MMT is $780\text{ m}^2\text{ g}^{-1}$ and that of the porous ceramic material is $31\text{ m}^2\text{ g}^{-1}$, which suggests that about 25 MMT plates are stacked together.

The OMLS consists of an octahedral $\text{AlO}_4(\text{OH})_2$ sheet sandwiched between two SiO_4 tetrahedral layers (of $\sim 1\text{ nm}$ thickness and $\sim 150\text{ nm}$ length) with charges being adjusted by substituting Al^{3+} or Si^{4+} with Mg^{2+} and depressed charges being neutralized with octadecylammonium cations intercalated into the interlayer spaces. The (020) plane of the individual silicate layers of the MMT is observed at $2\Theta \cong 19.7^{\circ}$ (cf. Figure 1C).

By contrast, for the porous ceramic material, the absence of clear Bragg diffraction peaks indicates that the crystal lattice of the OMLS has been completely destroyed in the porous ceramic material, as revealed by WAXD (Figure

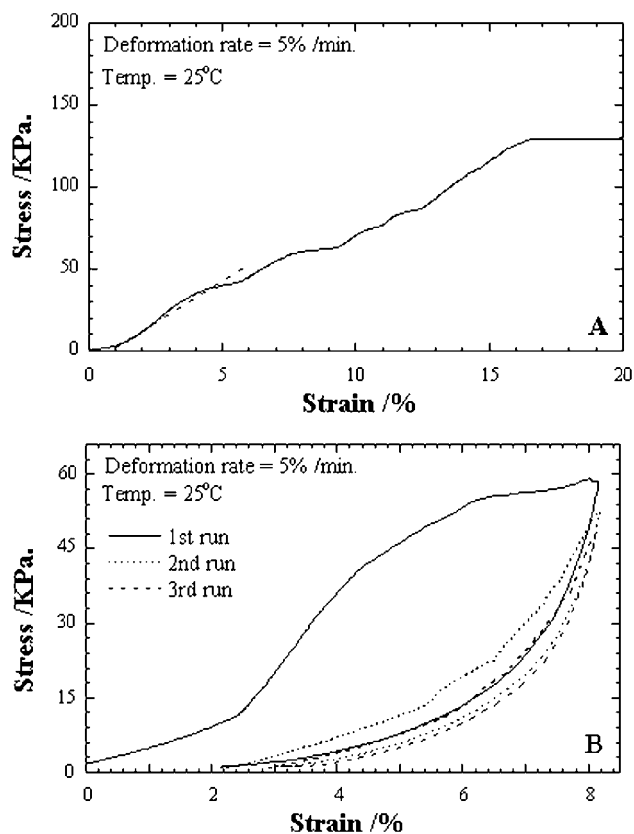


Figure 2. Stress–strain curve (A) and the strain recovery behavior (B) of the porous ceramic material under compression test. We conducted the compression test using the porous ceramic material of $2 \times 2 \times 1.5 \text{ mm}^3$ size.

1E).¹⁶ The formation of the house of cards structure in the material is presumably due to the complete degradation of intercalated PLA accompanied with the stacking of the platelet structure in the PLACN3. This degradation of PLA from a confined environment plays the important role of an adhesive between the platelets.

Figure 2 shows the stress–strain curve and the strain recovery behavior of the porous ceramic material by using a thermal mechanical analyzer (TMA4020S, MAC Science Co.) in the compression mode at a constant strain rate of $5\% \text{ min}^{-1}$. In the early stage, the compression stress increases with imposed strain, attains a certain level, and finally levels off at strain of 16% (cf. Figure 2A). The compression modulus, K , of the porous ceramic material was defined roughly by the initial slope of the stress–strain curve, as demonstrated by the broken line. The estimated rough value of K is in the order of $\sim 1.2 \text{ MPa}$, which is 5 orders of magnitude lower than the bulk modulus of MMT ($\sim 10^2 \text{ GPa}$).¹⁷ Note that the linear deformation behavior is nicely described in the early stage of the deformation, i.e., the deformation of the material closely resembles that of ordinary polymeric foams.¹ Figure 2B shows the characteristics feature of the stress–strain of compression and recovery behavior after unloading in the elastic region up to 8% strain. The residual

strain is 2% (first run), indicating that during compression, the local breakage of the weak points of both cells and house of cards structure takes place. For this reason, the initial and final parts of the strain–stress compression curve become flat somehow. After the first run, all of the weak points in the porous ceramic material are completely broken. On the second and third run, the porous ceramic material shows nice strain recovery behavior after unloading in the elastic region. This open-cell type porous ceramic material consisting of the house of cards structure is expected to provide the strain recovery and the excellent energy dissipation mechanism, probably with each plate bending like a leaf spring. This porous ceramic material is a new material possessing the features of elastic and very lightweight. This new route for the preparation of porous ceramic material via burning of nanocomposites can be expected to pave the way for a much broader range of applications for polymeric nanocomposites.

Acknowledgment. The present work was partially supported by the Grant-in-Aid for Academic Frontier Center under the project “Future Data Storage Materials” granted by the Ministry of Education, Science, Sports and Culture, Japan.

References

- (1) Gibson, L. J.; Ashby, M. F., Eds. *Cellular Solids*; Pergamon Press: New York, 1988, p 8.
- (2) Colombo, P.; Modesti, M. *J. Am. Ceram. Soc.* **1999**, *82*, 573.
- (3) Sepulveda, P.; Binner, J. G. P. *J. Eur. Ceram. Soc.* **1999**, *19*, 2059.
- (4) Smith, R. T.; Sambrook, R. M.; Binner, J. G. P. *Mater. Res. Soc. Symp. Proc.* **1995**, *371*, 297.
- (5) Nettleship, I. *Key Eng. Mater.* **1993**, *122*, 305.
- (6) Rice, R. W., Ed. *Porosity of Ceramics*; Marcel Dekker Inc.: New York, 1998, p 495.
- (7) Saggio-Woyansky, J.; Scott, C. E.; Minnear, W. P. *Am. Ceram. Soc. Bull.* **1992**, *71*, 1674.
- (8) Nangrejo, M. R.; Bao, X.; Edirisinghe, M. J. *Int. J. Inorganic Mater.* **2001**, *3*, 37, and references therein.
- (9) Messersmith, P. B.; Giannelis, E. P. *Chem. Mater.* **1994**, *6*, 1719.
- (10) Usuki, A.; Kawasumi, M.; Kojima, Y.; Okada, A.; Kurauchi, T.; Kamigaito, O. *J. Mater. Res.* **1993**, *8*, 1185.
- (11) Brown, J. M.; Curliss, D. B.; Vaia, R. A. *Proc. PMSE, Spring Meeting*, San Francisco, California, 2000, p 278–279.
- (12) Sinha Ray, S.; Maiti, P.; Okamoto, M.; Yamada, K.; Ueda, K. *Macromolecules* **2002**, *35*, in press.
- (13) Santis, P. De.; Kovacs, A. *Biopolymers* **1968**, *6*, 299.
- (14) We also burnt OMLS powder under the same conditions, but we got a lumpy white mass, with the exception of getting this type of porous material with a house of cards structure.
- (15) First we put a piece of porous ceramic material into hexane. It has a density (0.66 g/mL) between MMT (2.5 g mL^{-1}) and porous ceramic material, and then we made the system under reduced pressure ($\sim 150 \text{ mmHg}$). It initially floated on hexane, and some bubbles came out under reduced pressure. It finally sank into the hexane. This behavior indicates that porous ceramic material consists of open-cell structure.
- (16) When MMT is heated above $700 \text{ }^\circ\text{C}$ (but below $960 \text{ }^\circ\text{C}$), the first thing to happen is that all of the OH groups are eliminated from the structure, and thus, MMT is decomposed into that of a non-hydrated aluminosilicate. This transformation radically disturbs the crystalline network of the MMT, and the resulting diffraction pattern is indeed often typical of an amorphous (or noncrystalline) phase (Figure 1E).
- (17) Okamoto, M.; Morita, S.; Kim, Y. H.; Kotaka, T.; Tatayama, H. *Polymer* **2001**, *42*, 1201.

NL020284G